

Cluster model interpretation of normal and superdeformed bands in ^{60}Zn

B. Buck and A. C. Merchant

Department of Physics, University of Oxford, Theoretical Physics, 1 Keble Road, Oxford OX1 3NP, United Kingdom

S. M. Perez

Department of Physics, University of Cape Town, Private Bag, Rondebosch 7700, South Africa

(Received 21 July 1999; published 20 December 1999)

The ground state normal deformed band and the recently discovered superdeformed band in ^{60}Zn can be well described by treating them as $^{56}\text{Ni} + \alpha$ and $^{32}\text{S} + ^{28}\text{Si}$ cluster structures, respectively. In addition, the quadrupole deformation of the superdeformed band is reproduced satisfactorily.

PACS number(s): 21.60.Gx, 23.20.Js, 27.50.+e

Discrete γ -rays characteristic of superdeformation, in which the major to minor axis ratio of a deformed nucleus with axial symmetry is of order 2:1, were first observed in ^{152}Dy in 1986 by Twin *et al.* [1]. Since then, many more superdeformed bands have been found in four distinct regions of the Periodic Table, near $A = 80, 130, 150,$ and 190 [2]. Theoretical treatments employing the macroscopic-microscopic method of Strutinsky [3] in the range $42 \leq Z \leq 92$ are in general agreement with these observations and demonstrate that superdeformation should be a rather widespread phenomenon. Svensson *et al.* [4] have recently reported the discovery of a superdeformed (SD) band in ^{60}Zn (with a transition quadrupole moment of $2.75 \pm 0.45 e b$) and they were able to assign spin-parity values ranging from 8^+ to 30^+ to the member states. In addition, the ground state or normal deformed (ND) band of ^{60}Zn is established up to spin-parity 8^+ [4,5]. Here, we point out that the properties of both these bands can be understood within a cluster model of ^{60}Zn by assigning a $^{56}\text{Ni} + \alpha$ structure to the ND-band and a $^{32}\text{S} + ^{28}\text{Si}$ structure to the SD-band.

We have recently proposed [6] that likely binary clusterizations of a given parent nucleus can be identified by consideration of the local maxima of the function $D(Z_1, A_1, Z_2, A_2)$ defined by

$$D(Z_1, A_1, Z_2, A_2) = [B_E(Z_1, A_1) - B_L(Z_1, A_1)] + [B_E(Z_2, A_2) - B_L(Z_2, A_2)], \quad (1)$$

where B_E is an experimentally determined binding energy, and B_L the corresponding liquid drop value for each of the fragments of (charge, mass) (Z_i, A_i) with $i = 1, 2$ into which the parent of (charge, mass) (Z_T, A_T) may be divided. This corresponds to the largest deviations of the summed binding energies of the two fragments from liquid drop values. A convenient form for B_L is [7]

$$B_L = a_v A - a_s A^{2/3} - a_c \frac{Z^2}{A^{1/3}} - a_a \frac{(A - 2Z)^2}{A} + \delta, \quad (2)$$

where

$$\begin{aligned} a_v &= 15.56 \text{ MeV}, & a_s &= 17.23 \text{ MeV}, \\ a_c &= 0.697 \text{ MeV}, & a_a &= 23.285 \text{ MeV}. \end{aligned} \quad (3)$$

The pairing term δ in Eq. (2) is taken as $12/\sqrt{A}$ MeV because we consider only the fragmentation of even-even nuclei into even-even fragments. In addition, electric dipole transitions in even-even $N = Z$ nuclei are expected to be very weak suggesting that attention should be restricted to fragments obeying the condition

$$\frac{Z_1}{A_1} = \frac{Z_2}{A_2} = \frac{Z_T}{A_T}, \quad (4)$$

so that the implied dipole transition rates, which involve the operator $(Z_1/A_1 - Z_2/A_2)$, vanish identically.

Implementation of this procedure clearly shows that $^{56}\text{Ni} + \alpha$ is the most favorable binary decomposition of ^{60}Zn . This is to be expected since it consists of an α -particle orbiting a doubly magic core; a combination which, wherever it occurs across the Periodic Table, is known to give a good description of the ground state band of the parent nucleus [8]. However, there is also a local maximum of $D(Z_1, A_1, Z_2, A_2)$ for fragmentation into $^{32}\text{S} + ^{28}\text{Si}$, which in our model corresponds to a superdeformed intrinsic state having axial symmetry and a major to minor axis ratio of about 2:1.

Our technique for generating likely cluster-core decompositions, summarized in Eqs. (1)–(4), is not restricted to even-even $N = Z$ nuclei. We have previously demonstrated that it may be generalized to arbitrary even-even nuclei by taking a mixture of cluster-core components weighted so that the overall centers of mass and charge coincide (a no-dipole constraint) [6,9]. In particular, the method may be applied to other even-even isotopes of Zn having $A > 60$. For these heavier isotopes the cluster masses increase with A , for both the cluster-core decompositions corresponding to ND bands and for those corresponding to SD bands, with a consequent increase of the moment of inertia of both bands. The result is a tightening of the ND spectra as A increases, with the SD bands much less affected. The cluster charges show a corresponding increase with A , with the $B(E2)$ strengths for the ND bands increasing more markedly, percentage-wise, than those for the SD bands. Qualitatively therefore, the features

of the ND and SD bands generated by the model for ^{60}Zn are repeated for the heavier even-even isotopes of Zn.

We have not as yet attempted cluster model calculations for odd- A nuclei in the mass $A \sim 60$ region. We do not however foresee any difficulty in principle in carrying these out by coupling an extra nucleon to the ND and SD cluster structures discussed above. There will of course be additional technical complications involving half-integer spins and pairing, but we have already performed such calculations in the actinide region [10–13]. For the $A \sim 60$ region similar calculations would result in ND and SD bands of odd-even nuclei with moments of inertia and in-band $B(E2)$ strengths mirroring those of the underlying even-even bands. We now proceed to calculate the consequences of these suggestions for ^{60}Zn in a unified manner and confront them with the available data.

We employ a local potential in the Schrödinger equation for the relative motion of cluster and core, and interpret the solutions as bound or quasibound states of the parent nucleus. We have previously proposed a universal form for the cluster-core potential to be used for any arbitrary pair of fragments [14]

$$V(r) = V_0 \left(\frac{A_1 A_2}{A_1 + A_2 - 1} \right) \frac{f(r, R, x, a)}{f(0, R, x, a)}, \quad (5)$$

where

$$f(r, R, x, a) = \left[\frac{x}{\{1 + \exp[(r-R)/a]\}} + \frac{1-x}{\{1 + \exp[(r-R)/3a]\}^3} \right], \quad (6)$$

with specific parameter values

$$V_0 = 54.0 \text{ MeV}, \quad x = 0.33, \quad a = 0.73 \text{ fm}. \quad (7)$$

The radius R is chosen to reproduce the Q value for the separation of a known state of the parent nucleus into cluster and core components. (Here we choose the 4^+ state for the ND-band and the 10^+ state for the SD-band.) The Coulomb potential is taken as that for a point cluster interacting with a uniformly charged spherical core with radius $R_c = R$.

The Pauli principle requires all cluster nucleons to occupy states above the Fermi level of the core. We enforce this constraint by suitable choices of the cluster-core relative motion quantum numbers n (node number) and l (orbital angular momentum). For $^{56}\text{Ni} + \alpha$ we take $2n + l = G = 12$, which gives all the cluster nucleons three quanta each, consistent with their being in the (fp) shell, outside the $Z = N = 28$ subshell closure (and having no internal quanta). For $^{32}\text{S} + ^{28}\text{Si}$ we could share the cluster nucleons between the remainder of the (sd) shell and the (fp) shell. After allowing for the 36 internal quanta of a ^{28}Si cluster this would yield $G = 40$. However, splitting the ^{28}Si nucleons between differ-

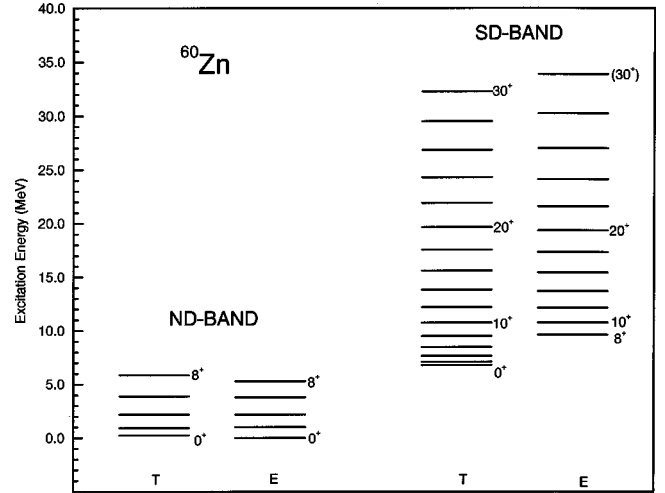


FIG. 1. Comparison of theoretical (T) and experimental (E) excitation energies of the states in the normal deformed (ND) and superdeformed (SD) bands of ^{60}Zn .

ent major shells is not a good way to form a cluster, and so we place all 28 nucleons in the (fp) shell, and subtract the internal quanta to find $2n + l = G = (3 \times 28) - 36 = 48$, consistent with an underlying oscillator shell model. The above procedure then results in values for R of 4.209 fm for $^{56}\text{Ni} + \alpha$ and 3.687 fm for $^{32}\text{S} + ^{28}\text{Si}$.

For a given cluster-core decomposition of a specified nucleus a strict application of the Wildermuth condition yields an approximate lower bound on the value of G describing the relative motion. The value obtained is independent of what one regards as the cluster or the core in the decomposition. In the present case this would yield $G = 12$ for the ND band and $G = 40$ for the SD band. These values can be regarded as a reasonable zeroth-order approximation. We find that $G = 12$ and $G = 48$ best reproduce the data. Although we have proposed a microscopic argument to support the choice of $G = 48$ for a ^{32}S core and ^{28}Si cluster, it is more profitably regarded as a parameter to be determined phenomenologically. We note that a similar microscopic argument applied to a ^{28}Si core and ^{32}S cluster would suggest $G = 52$, which makes very little difference to our calculations.

Figure 1 compares the calculated and observed energies for states up to 8^+ in the ground state ND band (which we predict to terminate at 12^+) and up to 30^+ in the SD band. The level of agreement is generally good, and the very much larger moment of inertia of the SD band arises naturally from the choice of similar masses for the cluster and core. We predict the 0^+ head of the SD band to be at an excitation energy of 6.80 MeV and the 10^+ member of the $^{56}\text{Ni} + \alpha$ ND band to be at 7.96 MeV. In addition to the superdeformed 10^+ state at 10.756 MeV, the experimental spectrum contains two other 10^+ states at 8.476 MeV and 8.636 MeV. These are so close together that they are likely to be substantially mixed. Thus although both of them are in the general vicinity of the predicted ND-band 10^+ member, neither of them will be a good candidate for pure $^{56}\text{Ni} + \alpha$ cluster structure, and so they are omitted from the spectrum comparison.

TABLE I. Calculated electric quadrupole strengths in the SD band of ^{60}Zn .

J	$B(E2; J \rightarrow J-2)$ (e b)	Q_t (e b)	β_2
2	0.180	3.01	0.51
4	0.257	3.00	0.51
6	0.281	3.00	0.51
8	0.292	2.99	0.51
10	0.296	2.97	0.50
12	0.296	2.94	0.50
14	0.293	2.91	0.49
16	0.288	2.87	0.49
18	0.280	2.82	0.48
20	0.270	2.76	0.47
22	0.258	2.69	0.46
24	0.245	2.62	0.45
26	0.230	2.53	0.44
28	0.213	2.43	0.42
30	0.195	2.33	0.41

We can also examine the electromagnetic properties of the states using the wave functions generated by our solutions of the Schrödinger equation. The $B(E2\downarrow)$ transition strengths may be calculated from

$$B(E2; J \rightarrow J-2) = \frac{15\alpha_2^2}{8\pi} \frac{J(J-1)}{(2J-1)(2J+1)} \langle r^2 \rangle^2 e^2 \text{fm}^4, \quad (8)$$

where $\langle r^2 \rangle$ is the integral of the square of the cluster-core separation distance r multiplied by the initial and final state wave functions and

$$\alpha_2 = \frac{Z_1 A_2^2 + Z_2 A_1^2}{(A_1 + A_2)^2}, \quad (9)$$

where Z_i and A_i are the cluster and core charges and masses, respectively. An effective charge ϵ may be introduced by replacing Z_i by $Z_i + \epsilon A_i$, and here we use $\epsilon = 0.1$ throughout consistent with the small values found in our previous applications of the cluster model. For the ND band we predict that $B(E2; 2^+ \rightarrow 0^+) = 132 e^2 \text{fm}^4 = 9.5 \text{ W.u.}$ For the SD band the experimental value for the transition quadrupole moment [4] of $2.75 \pm 0.45 e b$ should be compared with the values listed in Table I which are related to the $B(E2\downarrow)$ strengths by

$$eQ_t = \sqrt{\frac{32\pi \times (2J-1)(2J+1) \times B(E2; J \rightarrow J-2)}{15 \times J(J-1)}}. \quad (10)$$

In addition, we may relate these values to the deformation parameter β_2 of a uniform charge distribution, of shape $R = R_0(1 + \beta_2 Y_{20})$, which yields the same transition rates. We take $R_0 = 1.2A^{1/3} \text{ fm}$. To second order we find [15]

$$Q_t = \frac{3ZR_0^2}{\sqrt{5\pi}} (\beta_2 + 0.36\beta_2^2), \quad (11)$$

yielding values from our calculations of $0.41 \leq \beta_2 \leq 0.51$ (as J decreases from 30 to 2) to be compared with the experimental value of 0.47 ± 0.07 [4].

Satisfactory descriptions of ^{60}Zn in terms of the configuration-dependent shell-correction approach with the cranked Nilsson potential [16] and the cranked relativistic mean field formalism [17] are quoted by Svennson *et al.* [4]. We can see no obvious connection between these calculations and our own. However, our model should be judged according to its ability to reproduce experimental data, rather than by comparison with other models. This notwithstanding, a common point of the various models is that they suggest the coexistence of highly dissimilar intrinsic deformations in certain nuclei. Our criterion for selecting likely cluster-core decompositions gives rise to competing clusterizations involving widely varying cluster-core mass ratios. In a cluster model these generate very different deformations; small ratios corresponding to ND bands, and ratios of order unity to SD bands.

Using a local potential cluster model, with a universal form for the cluster-core potential, we have given a good account of the energies of the ground state (ND) band by treating it as a $^{56}\text{Ni} + \alpha$ system and of the excited superdeformed (SD) band by treating it as a $^{32}\text{S} + ^{28}\text{Si}$ system. The very different moments of inertia of these two bands are reproduced naturally and in an intuitively appealing way by these different choices of clusterization. In addition, the quadrupole deformation of the SD band is well described in our model using a small value of the effective charge.

A.C.M. would like to thank the U.K. Engineering and Physical Science Research Council (EPSRC) for financial support. S.M.P. would like to thank the S.A. Foundation for Research, and the University of Cape Town, for financial support.

- [1] P.J. Twin *et al.*, Phys. Rev. Lett. **57**, 811 (1986).
[2] B. Singh, R.B. Firestone, and S.Y. Frank Chu, Nucl. Data Sheets **78**, 1 (1996).
[3] T.R. Werner and J. Dudek, At. Data Nucl. Data Tables **50**, 179 (1992); **59**, 1 (1995).
[4] C.E. Svennson *et al.*, Phys. Rev. Lett. **82**, 3400 (1999).
[5] M.M. King, Nucl. Data Sheets **69**, 1 (1993).
[6] B. Buck, A.C. Merchant, and S.M. Perez, Few-Body Syst.

(to be published).

- [7] W.S.C. Williams, *Nuclear and Particle Physics* (Clarendon, Oxford, 1991), p. 60.
[8] B. Buck, A.C. Merchant, and S.M. Perez, Phys. Rev. C **51**, 559 (1995).
[9] B. Buck, A.C. Merchant, M.J. Horner, and S.M. Perez, Phys. Rev. C (to be published).
[10] B. Buck, A.C. Merchant, and S.M. Perez, Nucl. Phys. **A634**,

- 15 (1998).
- [11] B. Buck, A.C. Merchant, and S.M. Perez, Phys. Rev. C **58**, 2990 (1998).
- [12] B. Buck, A.C. Merchant, and S.M. Perez, Nucl. Phys. **A644**, 306 (1998).
- [13] B. Buck, A.C. Merchant, and S.M. Perez, Nucl. Phys. **A650**, 37 (1999).
- [14] B. Buck, A.C. Merchant, and S.M. Perez, Nucl. Phys. **A614**, 129 (1997).
- [15] B. Buck, A.C. Merchant, and S.M. Perez, Nucl. Phys. **A617**, 195 (1997).
- [16] T. Bengtsson and I. Ragnarsson, Nucl. Phys. **A436**, 14 (1985).
- [17] A.V. Afanasjev, J. König, and P. Ring, Nucl. Phys. **A608**, 107 (1996).